Highly Efficient Warm White Organic Light-Emitting Diodes by Triplet Exciton Conversion

Yi-Lu Chang, Yin Song, Zhibin Wang, Michael G. Helander, Jacky Qiu, Lily Chai, Zhiwei Liu, Gregory D. Scholes,* and Zhenghong Lu**

White organic light-emitting diodes (WOLEDs) are currently under intensive research and development worldwide as a new generation light source to replace problematic incandescent bulbs and fluorescent tubes. One of the major challenges facing WOLEDs has been to achieve high energy efficiency and high color rendering index simultaneously to make the technology competitive against other alternative technologies such as inorganic LEDs. Here, an all-phosphor, four-color WOLEDs is presented, employing a novel device design principle utilizing molecular energy transfer or, specifically, triplet exciton conversion within common organic layers in a cascaded emissive zone configuration to achieve exceptional performance: an 24.5% external quantum efficiency (EQE) at 1000 cd/m^2 with a color rendering index (CRI) of 81, and an EQE at 5000 cd/m^2 of 20.4% with a CRI of 85, using standard phosphors. The EQEs achieved are the highest reported to date among WOLEDs of single or multiple emitters possessing such high CRI, which represents a significant step towards the realization of WOLEDs in solid-state lighting.

Introduction

White organic light-emitting diodes (WOLEDs) are considered the most promising technology for next generation solid-state lighting due to their many attributes such as high energy efficiency, eye-friendly diffusive warm light, ultrathin form factor, etc. To produce high efficiency WOLEDs, the use of phosphors has become indispensable owning to their ability to generate light from both singlet and triplet excitons, thereby achieving nearly 100% internal quantum efficiencies.[1–3] In addition to high efficiency, a high color rendering capability for objects viewed under such white illumination source is another equally important parameter for solid-state lighting. In particular, a color rendering index (CRI) of over 80 is required to qualify WOLEDs as suitable illumination sources. To increase CRI, a number of groups have developed hybrid WOLEDs by employing a blue fluorophore along with green and red phosphors.[4–6] Schwartz et al.[5] have employed a blue fluorophore *N,N*′-di-1-naphthalenyl-*N,N*′-diphenyl-[1,1′:4′,1″:4″,1‴-quaterphenyl]-4,4‴-diamine (4P-NPD) together with a green and an orange phosphor to fabricate WOLEDs having a power efficiency at 1000 cd/m^2 ($\eta_{p,1000}$) of 37.5 lm/W, an external quantum efficiency (EQE_{1000}) of 16.1%, and a CRI of 86. More recently, Chen et al.[6] have employed 4,4′-bis(9-ethyl-3-carbazovinylene)-1,1′-biphenyl (BCzVBi) as the blue fluorophore along with a yellowish-green and a red phosphor to obtain a $\eta_{p,1000}$ of 11.3 lm/W, an EQE_{1000} of 10.7%, and a CRI of 91.2. Here, high CRI values are achieved at a cost of lower device efficiency.

To increase the device efficiency, several groups have taken the approach of using only two phosphorescent emitters to achieve very high efficiencies.[7–9] Su et al.[7] have reported a two-color WOLED employing a blue and an orange phosphor together with a carrier and exciton confining design to achieve high $\eta_{p,1000}$ and EQE_{1000} of 44.0 lm/W and 25.0%, respectively. Wang et al.[8] have incorporated a fluoro-modified iridium (III) bis(2 phenylbenzothiozolatoN,C$^{2'}$)(acetylacetonate) [Ir(BT)$_2$(acac)] yellow phosphor together with a blue phosphor to obtain a maximum power efficiency ($\eta_{p,max}$) of 34.0 lm/W and external quantum efficiency (EQE_{max}) of 26.2%. While high in energy efficiency, these devices have extremely low CRI (<70) which is insufficient for illumination sources.[7–9] Therefore, the use of three or more phosphorescent emitters has become a prerequisite for high color-rendering and highly efficient lighting applications.[10–12]

To solve this problem, the current prevailing wisdom has been designing WOLEDs by co-doping multiple phosphorescent emitters with different colors into one emissive layer (EML), i.e., as a single unit, while preserving all emission colors with the advantage of having a reduced total number of organic layers.[2,13–16] However, such approach makes it more difficult to tune the emission spectrum as most of the energy will naturally transfer to the lower energy emitters. This typically results in the use of

Y.-L. Chang, Z. Wang, M. G. Helander, J. Qiu, L. Chai, Dr. Z. Liu, Prof. Z. Lu
Department of Materials Science and Engineering
University of Toronto
184 College St., Toronto, Ontario, M5S 3E4, Canada
E-mail: yilu.chang@mail.utoronto.ca;
zhenghong.lu@utoronto.ca

Y. Song, Prof. G. D. Scholes
Department of Chemistry
Institute for Optical Science and Center for Quantum Information and Quantum Control University of Toronto
80 St George Street, Toronto, Ontario,
M5S 3H6, Canada
E-mail: greg.scholes@utoronto.ca

DOI: 10.1002/adfm.201201858

high concentration high energy dopants (e.g., blue phosphors) and low concentration low energy dopants (e.g., red phosphors) with respect to the host,[13,14,16,17] which further limits the degree of control over the emission efficiency for each color.

In this work, we demonstrated all-phosphor, four-color (i.e., blue, green, yellow, and red emissions) WOLEDs with high efficiencies and high CRI values. These WOLEDs are designed and constructed based on molecular energy transfer or, more specifically, triplet exciton conversion (TEC) process, where the emission efficiency of yellow $Ir(BT)_2(acac)$[18] and red iridium (III) bis(2-methyldibenzo[f,h]quinoxaline)(acetylacetonate) $[Ir(MDQ)_2(acac)]$[19] phosphors are significantly enhanced by inclusion of a TEC green phosphor, respectively. Detailed analysis showed that this enhancement in efficiency is attributed to effective exciton gathering by the green phosphor followed by efficient energy transfer to an emitter having a lower energy. To quantify the quantum mechanical process, we employed time-correlated single photon counting (TCSPC) technique and realized a high energy transfer efficiency of over 90% from the green to red and yellow phosphors. Based on the TEC process, we have designed and fabricated WOLEDs with exceptional performance: an EQE_{1000} of 24.5% with a CRI of 81, and an EQE_{5000} of 20.4% with a CRI of 85, using well-known green and blue emitters, namely, iridium (III) bis(2-phenylpyridine)-(acetylacetonate) $[Ir(ppy)_2(acac)]$[1,20] and iridium (III) bis(4,6-difluorophenyl-pyridinato-N,$C2'$)(picolinate) [FIrpic].[7,21] The EQEs achieved represent the highest reported to date among WOLEDs of single or multiple emitters possessing such high CRI.

2. Results and Discussion

2.1. WOLEDs Design and Performance Characterization

Figure 1a shows a schematic illustration of four WOLED device structures (W1–W4) used in this work, and Figure 1b shows the corresponding energy level diagram. In each device,

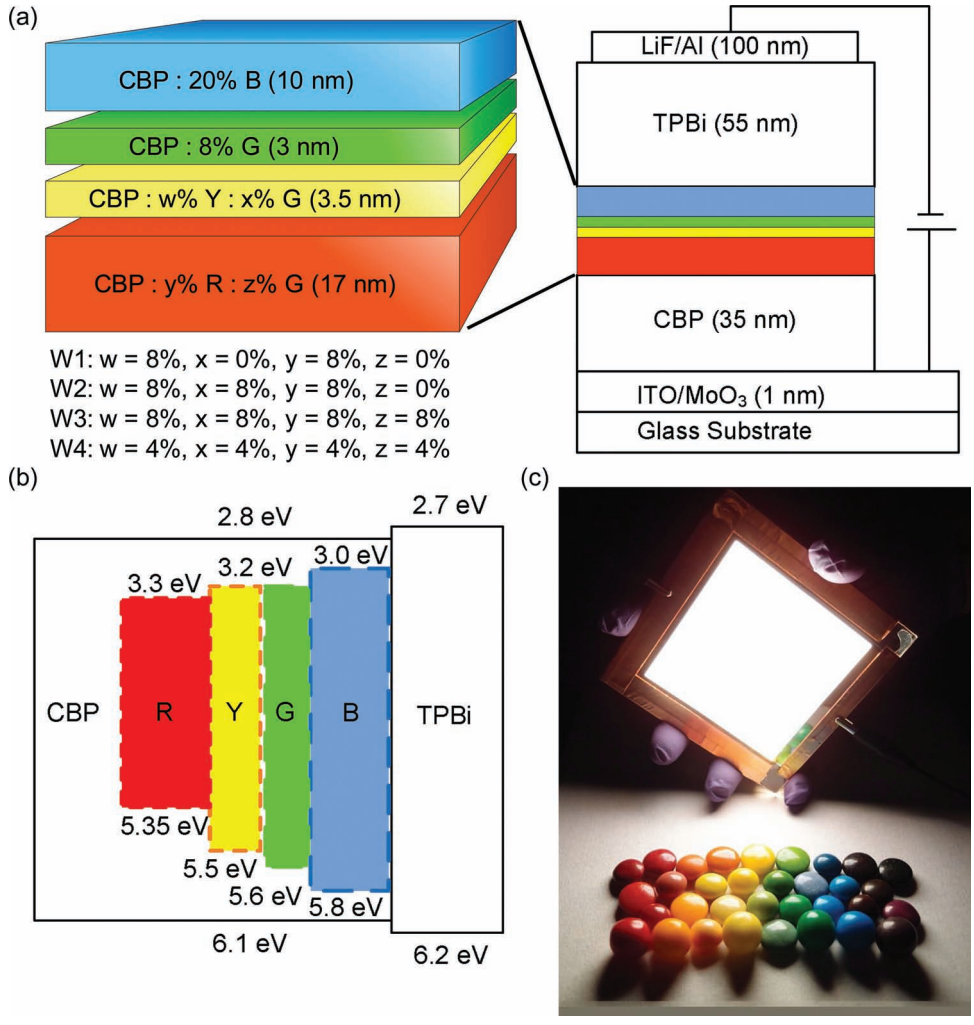

Figure 1. Device configurations (a) and energy level diagrams (b) for WOLEDs W1–W4. The dopants employed are FIrpic for blue (B), $Ir(ppy)_2(acac)$ for green (G), $Ir(BT)_2(acac)$ for yellow (Y), and $Ir(MDQ)_2(acac)$ for red (R). All doping concentrations are in wt%. c) A photo of a large area (80 mm × 80 mm) WOLED (W3) illuminating at 5000 cd/m^2 with a color rendering index of 85.

TPBi [2,2′,2″-(1,3,5-benzinetriyl)-tris(1-phenyl-1-H-benzimidazole)] serves as the electron transport layer (ETL), and CBP [4,4′-bis(carbazol-9-yl)biphenyl] functions as a hole transport layer (HTL) and as a triplet host. ITO/MoO_3 anode and LiF/Al cathode are applied. In this configuration, the majority of excitons will be generated near the CBP/TPBi interface (on both sides) before being harvested by the emitters (i.e., recombination occurs) on the CBP side. Further, as both CBP and TPBi are wide energy gap materials with high triplet energies,[22] the generated excitons can be well-confined onto the emitters. Since the blue emitter, FIrpic, has the closest energy levels to both materials,[22] direct exciton formation on the blue dopant is unlikely and it is critical to place the blue emitter closest to the CBP/TPBi interface to harvest excitons first. Other lower energy green, yellow and red emitters are placed sequentially next to blue to harvest excitons in a cascaded fashion as shown by the energy level diagram in Figure 1b. This cascaded design using a single host allows for only a single site for exciton generation and recombination without introducing other barrier layers (i.e., a second or third host material) that could induce undesirable charge accumulation in the device, leading to notorious triplet-polaron and polaron-polaron quenching processes.[23–25] It is also important that there is no interlayer between two adjacent emitting layers so that the surplus excitons can readily diffuse into the adjacent layer with an emitter having a lower energy. This inter-zone free flow of excitons is in stark contrast to the widely accepted design involving the use of interlayers,[4,11] and is key to maximize our device overall quantum efficiency. To demonstrate this point, we have fabricated a series of devices with one emitter (blue), two emitters (blue and green), three emitters (blue, green, and yellow), and four emitters (blue, green, yellow, and red) as shown in **Figure 2**. We found that with each additional emitter incorporated, the EQE progressively improves from 8.5% to 19.2% as the emissive zone increases from one to four, respectively. In particular, we observe that for blue doped only device, the emission efficiency is fairly low (<10%), indicating that a considerable portion of the excitons are not being transferred from CBP to FIrpic. However, with the inclusion of a green doped region adjacent to the blue doped region, the device shows a nearly twofold increase in efficiency without sacrificing the emission from FIrpic, which demonstrates that the energy transfer from CBP to FIrpic, and then to the adjacent $Ir(ppy)_2(acac)$ is less significant compared to direct CBP energy transfer to the $Ir(ppy)_2(acac)$ after exciton diffusion in host CBP from blue to green doped region. This shows that excitons generated near the CBP/TPBi interface are effectively harvested by the cascaded emission zones.

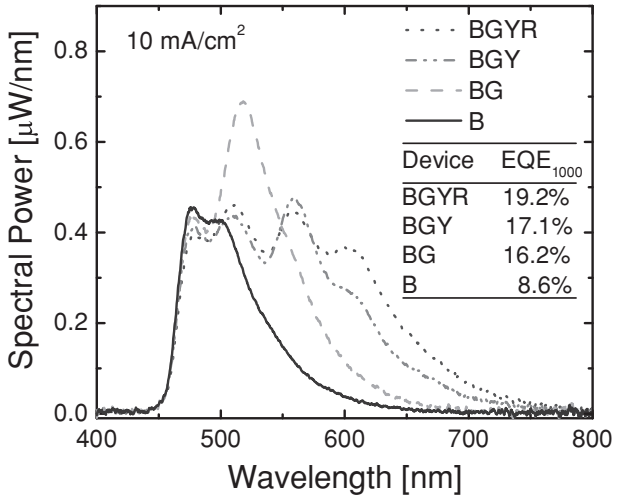

Figure 2. Spectral power spectra at 10 mA/cm² with a progressive addition of each emissive layer to construct W1. Inset shows EQE of devices at a luminance of 1000 cd/m². The dopants used are FIrpic for blue (B), $Ir(ppy)_2(acac)$ for green (G), $Ir(BT)_2(acac)$ for yellow (Y), and $Ir(MDQ)_2(acac)$ for red (R). Each device layer thicknesses and doping concentrations are as shown for W1 in Figure 1.

A summary of device performance is listed in **Table 1**, and the power efficiency-luminance-external quantum efficiency (PE-L-EQE) characteristics as well as the corresponding electroluminance (EL) spectrum (insets) of each device are shown in **Figure 3**. The inter-zone exciton harvesting concept led to device W1 with decent EQE_{100} ($\eta_{p,100}$) and EQE_{1000} ($\eta_{p,1000}$) of 16.8% (32.1 lm/W) and 19.2% (28.1 lm/W), respectively. The high efficiency at high luminance is mainly due to the elimination of accumulated carriers across the entire device, i.e., the unique design of using CBP as both the host and HTL, which has been demonstrated in our previous work.[20] Also noted is the spectral shift with a reduction in blue emission and improvement in yellow and red emissions at higher luminance as shown in the inset of Figure 3a. This can be attributed to a shift of the exciton generation towards the yellow and red doped regions at higher driving voltages. Since CBP can also transport electrons quite efficiently, at a higher driving voltage, relatively more electrons can be injected deeper into the CBP side to form excitons in the

Table 1. Summary of WOLED performances.

Device	$\eta_{p,100}/\eta_{c,100}/EQE_{100}$ [a)] [lm W^{-1}/cd A^{-1}/%]	$\eta_{p,1000}/\eta_{c,1000}/EQE_{1000}$ [b)] [lm W^{-1}/cd A^{-1}/%]	$\eta_{p,5000}/\eta_{c,5000}/EQE_{5000}$ [c)] [lm W^{-1}/cd A^{-1}/%]	CRI [d)]	$CIE_{(x,y)}$ [e)]
W1	32.1/39.2/16.8	28.1/44.8/19.2	20.5/41.5/17.8	71,72	(0.37,0.48)
W2	37.3/45.6/19.1	32.2/50.2/21.0	23.1/46.0/19.2	70,69	(0.38,0.48)
W3	40.5/53.7/23.0	31.0/53.9/23.3	20.8/47.0/20.4	84,85	(0.44,0.45)
W4	42.6/55.1/23.5	33.8/57.7/24.5	23.2/51.2/21.9	81,82	(0.44,0.46)

[a)]Power efficiency (PE), current efficiency (CE), and external quantum efficiency (EQE) at 100 cd/m²; [b)]PE, CE, and EQE at 1000 cd/m²; [c)]PE, CE, and EQE at 5000 cd/m²; [d)]Color rendering index at 1000 cd/m² and 5,000 cd/m²; [e)]Commission Internationale de L'Eclairage coordinates at 5000 cd/m².

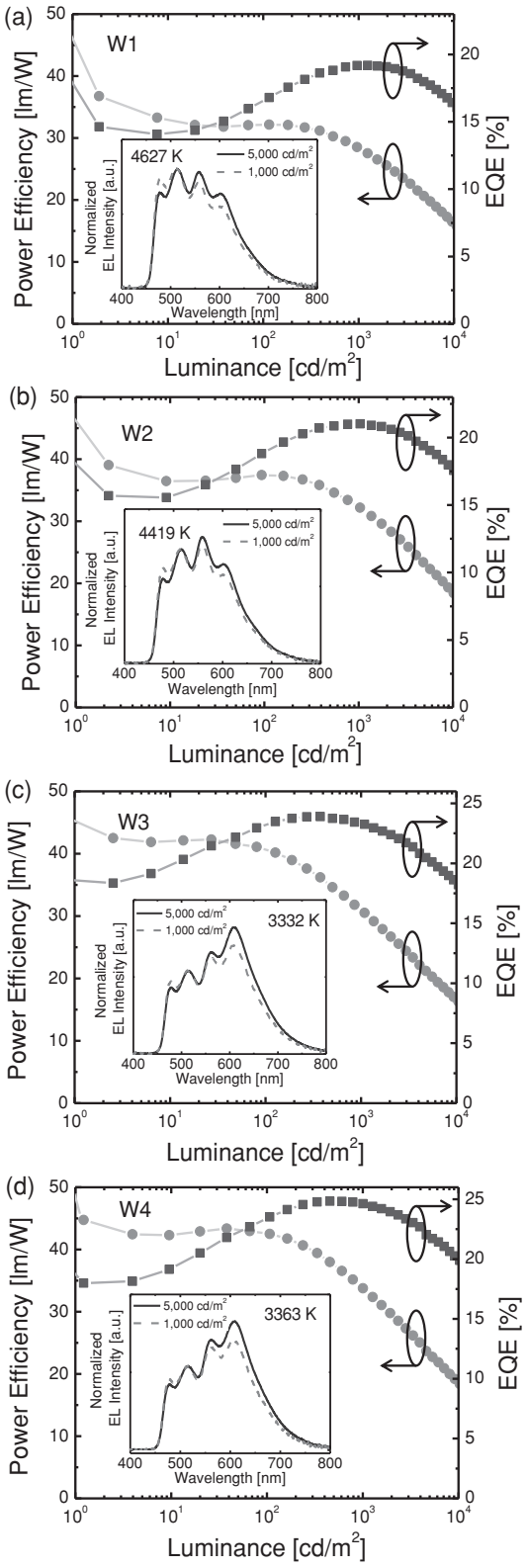

Figure 3. a–d) PE-L-EQE characteristics of the WOLED devices considered in this work. The insets show the corresponding electroluminance (EL) spectra under various luminances normalized to the green emission peak at 520 nm.The correlated color temperature (CCT) at a luminance of 5000 cd/m^2 for each device is also shown in the inset.

host which are subsequently transferred to the yellow and red dopants, resulting in the emission intensity enhancement.

In order to further improve upon the efficiency of the device, we incorporated a higher energy (green) phosphor into the yellow emissive layer (W2) to enable intra-zone TEC, i.e., molecular energy transfer within a common emissive layer. From our previous study on single color red OLED devices, we learned that incorporation of the green phosphor will improve the emission efficiency of a red OLED, while preserving the overall emission spectrum, i.e., the EL spectrum remains predominantly in red.[26] Similarly, it is apparent here that with the green phosphor incorporation in device W2, the yellow emission is significantly enhanced, becoming the dominant emission peak as shown in the inset of Figure 3b. This spectral intensity enhancement corresponds to a considerable improvement in EQE_{100} and EQE_{1000} to 19.1% (37.3 lm/W) and 21.0% (32.2 lm/W), respectively. However, devices W1 and W2 exhibit CRI values of only 71 and 70 (see Table 1), respectively, which do not qualify them as adequate illumination sources.

To improve the CRI, we incorporated the green phosphor into the red emissive layer in addition to the yellow emissive layer (W3). From the EL spectrum in the inset of Figure 3c, we observe the red emission at ≈610 nm becomes the most dominant peak, leading to a high CRI of 84 at 1000 cd/m^2. The green phosphor incorporation in the red emissive region also enhanced EQE_{100} and EQE_{1000} to 23.0% (40.5 lm/W) and 23.3% (31.0 lm/W), respectively. At a high luminance of 5000 cd/m^2 that is critical for solid-state lighting, the EQE remains as high as 20.4% with a high CRI of 85, Commission Internationale de L'Eclairage (CIE) coordinates of (0.44, 0.45) and a correlated color temperature (CCT) of 3332 K, corresponding to a desirable warm white illumination. To the best of our knowledge, this is the first report of a WOLED achieving EQE_{5000} of over 20% with a CRI of 85 in the scientific literature. A photo of a large area (80 mm × 80 mm) device, W3, illuminating on arrays of closely colored objects is shown in Figure 1c, where excellent color rendering capability is displayed by the fact that the color of each object can be clearly identified. To further relieve the triplet-triplet annihilation[23,25,27] and triplet-polaron quenching processes[23–25] at high luminance, we lowered the co-doping concentrations in both yellow and red emissive regions as demonstrated in W4. It is observed in Figure 3d that the spectrum is characterized by a slightly increased yellow emission compared to W3. Notably, the EQE_{100}, EQE_{1000} and EQE_{5000} have improved to 23.5% (42.6 lm/W), 24.5% (33.8 lm/W), and 21.9% (23.2 lm/W), respectively. Even at an ultrahigh luminance of 10 000 cd/m^2, the EQE remains as high as 20.1% with a CRI of 82. The EQEs achieved represent the highest reported to date among WOLEDs of single or multiple emitters exhibiting the corresponding decent CRI values in the scientific literature (Supporting Information, Table S1).

To reduce the loss in optical out-coupling, we used a simple lens-based out-coupling enhancement technique[11,28] and obtained $\eta_{p,100}$ (EQE_{100}), $\eta_{p,1000}$ (EQE_{1000}) and $\eta_{p,5000}$ (EQE_{5000}) of 76.0 lm/W (41.5%), 61.7 lm/W (44.3%) and 42.9 lm/W (40.6%), respectively, for W4. The corresponding CRI values are 81, 83, and 85, respectively (Supporting Information, Figure S1). The resulting efficiency enhancement factor was

≈1.8. These power efficiencies are in the range of standard fluorescent tubes (40–70 lm/W), but the color rendering index is far superior for lighting applications. We note that all results reported herein have been reproduced for multiple devices on the same substrate and in all cases the efficiencies are reproducible within 0.1%.

2.2. Device Working Principle

To investigate the working principle behind the performance improvement in these WOLEDs, we simplified the device structure by investigating the performance enhancement on one-color yellow and one-color red OLED devices while maintaining the same EML and transport layer thickness as in the WOLED devices. **Figure 4**a illustrates the spectral power, i.e., the total radiant power per wavelength, of the red device with and without green phosphor incorporation in the emissive layer. It is apparent that both spectra are characterized by a dominant red peak at ≈605 nm, but the device with green phosphor incorporation shows a significantly higher spectral power with an additional small peak attributed to the green phosphor emission (520 nm). More importantly, by examining the spectra closely (inset of Figure 4a), we observe a considerably higher host CBP emission from solely red doped device, indicating that the green phosphor can assist in trapping excitons or utilizing excitons formed in the CBP host more efficiently. This phenomenon is also observed for yellow emission devices (Supporting Information, Figure S2).

In addition, Figure 4b illustrates the photoluminance (PL) spectrum of the green phosphor and the absorption spectra of yellow and red phosphors in solution. It is clear that there is a substantial spectral overlap between the green phosphor triplet emission and the triplet metal-ligand-charge-transfer (^{3}MLCT) states absorption of both red and yellow phosphors, which ensures the efficient energy transfer cascade when the green phosphor is included in the device. This cascaded energy transfer evidently is quite long range, given the levels of phosphor doping in our devices. That suggests a Förster-type[29,30] mechanism is involved, either promoted by spin-orbit coupling[31] or allowed by angular momentum conservation.[32] We can therefore deduce that the efficiency enhancement is attributed to improved host exciton utilization by the green phosphor, followed by efficient triplet energy transfer from the green to lower energy yellow or red emitters as expressed by:

$$\eta_{ext} = \gamma \eta_{out} \chi \phi_{PL} \quad (1a)$$

$$= \gamma \eta_{out} \left\{ \chi_A \phi_{PL,A} + \chi_D \left[\eta_{D-A} \phi_{PL,A} + (1 - \eta_{D-A}) \phi_{PL,D} \right] \right\} \quad (1b)$$

where η_{ext} is the external quantum efficiency, γ represents charge balance factor, η_{out} is the out-coupling efficiency, χ denotes the fraction of emissive excitons that are trapped by the donor (χ_D) and acceptor molecules (χ_A), φ_{PL} is the quantum yields of the emitters, and $\eta_{D\text{-}A}$ stands for the energy transfer efficiency from donor (D) to acceptor (A), i.e., from green to yellow or red phosphors. Using Equation (1a) and device parameters from optimized single emitter devices, we can derive the fraction of emissive excitons trapped by each emitter, χ, to be ≈0.96, ≈0.87, and ≈0.77 for green, yellow and red devices, respectively (Supporting Information). Since the green emitter exhibits the highest exciton trapping capability in the device, it will be beneficial to incorporate it as co-doped EMLs to compensate for the relatively inferior trapping ability of yellow and red emitters and hence increase the utilization rate of the available excitons. This is also reflected from the current density versus voltage (J–V) plot of the WOLED devices as shown in Figure S3 (Supporting Information), where a reduction in current density is observed with the incorporation of the green emitter. This can be attributed to increased hole trapping by the green emitter, which leads to direct exciton formation and effective widening of the recombination zone, followed by efficient exciton energy transfer to the red and yellow emitters. According to Equation (1b), we can see that the presence of χ_D together with a high $\eta_{D\text{-}A}$ will result in an enhanced emission from the lower energy emitter. However, if $\eta_{D\text{-}A}$ is not sufficiently high, the χ_D may also contribute to green (donor) emission (≈520 nm) as shown in Figure 4a. In terms of our WOLED design, the green donor emission will nevertheless contribute favorably to overall device efficiency of W2 to W4.

In order to determine $\eta_{D\text{-}A}$, we have conducted time-correlated single photon counting (TCSPC) technique to

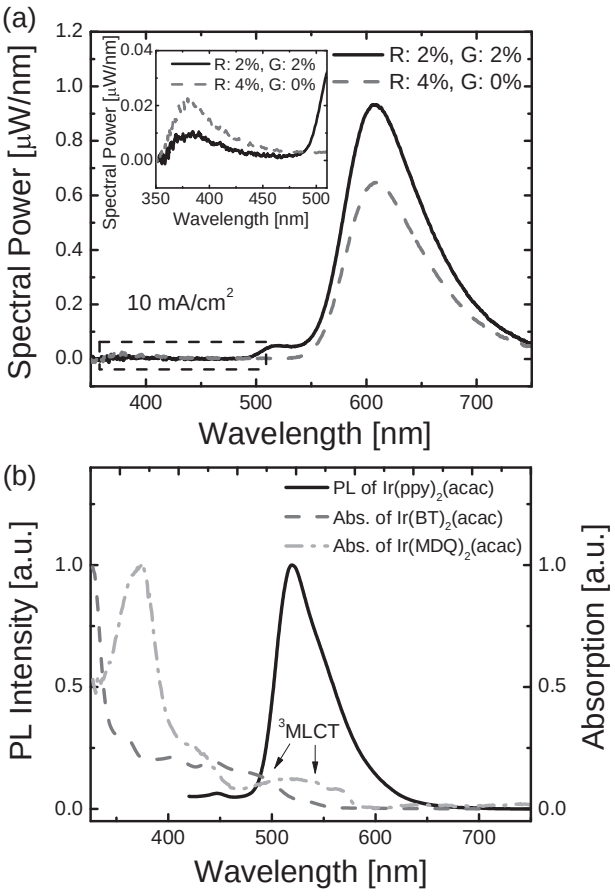

Figure 4. a) Spectral power spectra of co-doped and single-doped red emitting devices at 10 mA/cm^2. The inset shows the portion of the spectrum enclosed by the dashed box, which highlights host emission intensity with and without co-doping. b) PL emission spectra of Ir(ppy)$_2$(acac) and absorption spectra of Ir(BT)$_2$(acac) and Ir(MDQ)$_2$(acac) in CH_2Cl_2 (≈1×10^{-5} M).

measure the transient decay time of the donor emission at 520 nm under various co-doping concentrations for both red and yellow doped CBP films as shown in **Figure 5**. Control samples of green donor-doped only films at various concentrations (2%, 4%, 6%, and 8%) revealed similar decay time constants of ≈1.15–1.20 μs, which include both the nonradiative and radiative relaxation processes of the green donor triplet states. In co-doped films, we anticipate that any energy transfer from the green donor to either red or yellow acceptor molecules will induce an additional green donor triplet relaxation path, leading to a shorter decay time. We can therefore describe the transient donor emission intensity by:[33]

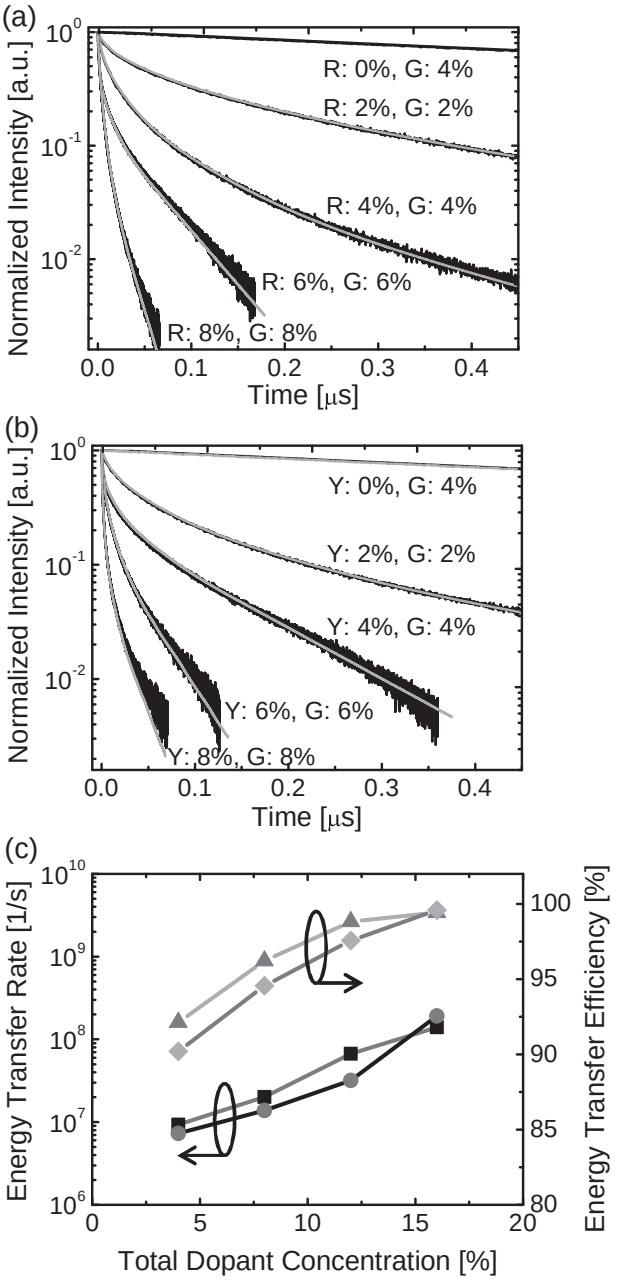

Figure 5. Solid state transient response of (a) red and green co-doped CBP films and (b) yellow and green co-doped CBP films at various co-doping concentrations. The solid lines are the exponential fits to the transient decay responses. The excitation wavelength is at 350 nm. c) Calculated energy transfer rate and efficiency versus total dopant concentration with the control sample concentration corresponding to the green donor concentration of the co-doped films. Triangles (squares) and rhombuses (circles) denote the energy transfer efficiency (energy transfer rate) of co-doped yellow and red emissive films, respectively.

$$l(t) = e^{-K_C t}(C_1 + C_2\, e^{-K_{et} t}) \tag{2}$$

where K_c represents the decay rate constant of the donor emission (from the control samples), k_{et} denotes the energy transfer rate from donor to acceptor, and C_1 and C_2 are related to the donor and acceptor concentrations, respectively. Using Equation (2), we can describe the transient response of the donor emission in co-doped films as illustrated in Figure 5a,b, and obtain the energy transfer rate as shown in Figure 5c. The energy transfer efficiency can then be expressed as:

$$\eta_{D-A} = \frac{k_{et}}{k_{et} + k_r + k_{nr}} = \frac{k_{et}}{k_{et} + K_c} \tag{3}$$

where the K_c term consists of the sum of radiative (k_r) and nonradiative (K_{nr}) rate constants of the donor triplet states of the control films. From Figure 5a,b, we can clearly observe for both red and yellow emissive films a faster transient decay with increasing co-doping concentration, which corresponds to a reduction in donor-to-acceptor molecule distance that promotes the energy transfer process. It is worth noting that in co-doped films, the transient decay response of the lower energy yellow and red emissions does not alter significantly compared to those from single doped yellow and red films, suggesting no other nonradiative energy transfer path took place. This is expected since any increase in the excited state population of the lower energy emitters should not affect their triplet radiative decay lifetimes. We also note that for high co-doping concentrations, an extra exponential term is included to account for donor-to-donor exciton diffusion[33] before eventually transferring to an acceptor, which is a relatively slower process (Supporting Information). As shown in Figure 5c, the η_{D-A} is calculated to be as high as ≈90.2 and ≈92.1% for red and yellow emissive films, respectively, at low co-doping concentrations (2% each). The η_{D-A} further reaches ≈99.6% and ≈99.4% for red and yellow emissive films, respectively, at high co-doping concentrations (8% each), which represents nearly perfect energy transfer. This high energy transfer efficiency together with an increased exciton utilization rate can well-explain the observed spectral EL intensity enhancement of the lower energy red and yellow emissions, and hence the overall device efficiency improvement of WOLEDs W2 to W4.

3. Conclusions

We reported a novel WOLED architecture based on the TEC process, where the efficiency and spectral intensity of the yellow and red emitters are significantly enhanced by facile energy transfer from a selected green phosphor with high exciton trapping capability. This intra-zone molecular energy transfer from high energy donor to low energy acceptor molecules was found to be over 90% efficient through a Förster-type transfer process. The enhancements in red emission also led to high CRI values

of 81–85, suitable for solid-state lighting. In essence, the TEC process provides an effective pathway in engineering the WOLED emission spectra, and consequently high CRI, while at the same time leading to a significantly improved WOLED efficiency. At a high luminance of 5000 cd/m^2, WOLEDs with an unprecedented EQE of 20.4% and a high CRI of 85 have been demonstrated. The CRI could further be improved with the use of higher efficiency deep blue emitters, which are mostly proprietary. Aided with a lens-based out-coupling enhancement, a high power efficiency of 76.0 lm/W was also obtained. This TEC concept does not require the use of exotic ultra-wide energy gap and associated ultra-high triplet energy host materials for the blue emitter, which is commonly believed to be a prerequisite for high efficiency WOLEDs.[13,34–38] The TEC concept could further spur the development of a new generation of low-cost WOLEDs by enabling the use of alternative, more abundant metal-organic complexes such as Pt-[39–41] or even Cu-based[42] emitters as low energy acceptor phosphors, provided the energy transfer process remains proficient.

4. Experimental Section

Device Fabrication and Characterization: All WOLEDs were fabricated by thermal evaporation using a Kurt J. Lesker LUMINOS cluster tool under a base pressure of ≈10^{-8} Torr on a glass substrate (1.1 mm thick) precoated with indium tin oxide (ITO), having a thickness and sheet resistance of 120 nm and 15 Ω/sq, respectively. Prior to loading, the substrate was degreased with standard solvents, blow-dried using a N_2 gun, and treated in a UV-ozone chamber. All doping concentration used in this work are by weight percentage. The active area for each device was ≈2 mm^2 as verified with an optical microscope. The deposited layer thickness was monitored by a quartz crystal microbalance that was calibrated by spectroscopic ellipsometry (Sopra GES 5E). All dopants were purified by gradient sublimation before use to ensure the highest purity possible. Precise control of layer thicknesses during the device fabrication as well as the purity of the phosphorescent emitter was found to be critical to obtaining highly efficient devices with high reproducibility. Luminance-voltage measurements were carried out using a Minolta LS-110 Luminance Meter. Current-voltage characteristics were measured using an HP4140B pA meter. The radiant flux for calculating EQEs was measured using an integrating sphere equipped with an Ocean Optics USB 4000 spectrometer with NIST traceable calibration using a halogen lamp.[43] Measurements with out-coupling enhancement used a 10 mm diameter BK7 half-sphere lens mounted on top of the device with index matching gel.[11,28] The geometry for the lens-based out-coupling enhancement measurement using an integrating sphere is shown in the Supporting Information (Figure S4).

PL Measurements: The solution PL measurements were conducted using Perkin Elmer LS55 fluorescence spectrometer and the absorption measurements were carried out using Perkin Elmer Lambda 25 UV-vIS spectrometer. The absolute quantum yield measurements were performed using a custom built setup according to the procedure reported in Ref.[44] A 365 nm collimated LED from Thorlabs (M365L2-C2) served as the excitation source, which was directed onto the sample consisted of a doped organic film (100 nm thick) deposited on a quartz substrate (1 mm thick) and mounted inside a calibrated integrating sphere. The light generated was then detected using an Ocean Optics Maya 2000 Pro spectrometer.

Transient Measurements: The TCSPC measurements were conducted using an IBH Datastation Hub system with an IBH 5000 M PL monochromator and an R3809U-50 cooled MCP PMT detector. The light source used was a model 3950 ps Ti: sapphire Tsunami laser (Spectra-Physics), pumped by a Millenium X (Spectra-Physics) diode laser, pulse picked (Model 3980 Spectra-Physics), and frequency doubled using a GWU-23PL multiharmonic generator (Spectra-Physics). Pulse repetition rates were kept below 100 kHz. The samples consisted of doped CBP films (50 nm thick) on quartz that were encapsulated with a second, identical sized, blank quartz using ultraviolet (UV)-sensitive epoxy under N_2 environment prior to measurement.

Supporting Information

Supporting Information is available from the Wiley Online Library or from the author.

Acknowledgements

The authors wish to acknowledge funding for this research from the Natural Sciences and Engineering Research Council (NSERC) of Canada. Z.H.L. is a Government of Canada Research Chair in Organic Optoelectronics, Tier I.

Received: July 5, 2012
Revised: August 21, 2012
Published online: September 17, 2012

[1] C. Adachi, M. A. Baldo, M. E. Thompson, S. R. Forrest, *J. Appl. Phys.* **2001**, *90*, 5048.
[2] J. H. Seo, S. J. Le, B. M. Seo, S. J. Moon, K. H. Lee, J. K. Park, S. S. Yoon, Y. K. Kim, *Org. Electron.* **2010**, *11*, 1759.
[3] M. A. Baldo, D. F. O'Brien, Y. You, A. Shoustikov, S. Sibley, M. E. Thompson, S. R. Forrest, *Nature* **1998**, *395*, 151.
[4] Y. R. Sun, N. C. Giebink, H. Kanno, B. W. Ma, M. E. Thompson, S. R. Forrest, *Nature* **2006**, *440*, 908.
[5] G. Schwartz, M. Pfeiffer, S. Reineke, K. Walzer, K. Leo, *Adv. Mater.* **2007**, *19*, 3672.
[6] S. M. Chen, G. P. Tan, W. Y. Wong, H. S. Kwok, *Adv. Funct. Mater.* **2011**, *21*, 3785.
[7] S. J. Su, E. Gonmori, H. Sasabe, J. Kido, *Adv. Mater.* **2008**, *20*, 4189.
[8] R. J. Wang, D. Liu, H. C. Ren, T. Zhang, H. M. Yin, G. Y. Liu, J. Y. Li, *Adv. Mater.* **2011**, *23*, 2823.
[9] B. H. Zhang, G. P. Tan, C.-S. Lam, B. Yao, C.-L. Ho, L. H. Liu, Z. Y. Xie, W.-Y. Wong, J. Q. Ding, L. X. Wang, *Adv. Mater.* **2012**, *24*, 1873.
[10] H. Sasabe, J.-I. Takamatsu, T. Motoyama, S. Watanabe, G. Wagenblast, N. Langer, O. Molt, E. Fuchs, C. Lennartz, J. Kido, *Adv. Mater.* **2010**, *22*, 5003.
[11] S. Reineke, F. Lindner, G. Schwartz, N. Seidler, K. Walzer, B. Lüssem, K. Leo, *Nature* **2009**, *459*, 234.
[12] Y. B. Zhao, J. S. Chen, D. G. Ma, *Appl. Phys. Lett.* **2011**, *99*, 163303.
[13] B. W. D'Andrade, R. J. Holmes, S. R. Forrest, *Adv. Mater.* **2004**, *16*, 624.
[14] Q. Wang, J. Q. Ding, D. G. Ma, Y. X. Cheng, L. X. Wang, F. S. Wang, *Adv. Mater.* **2009**, *21*, 2944.
[15] S. H. Eom, Y. Zheng, E. Wrzesniewski, J. Lee, N. Chopra, F. So, J. Xue, *Appl. Phys. Lett.* **2009**, *94*, 153303.
[16] C. H. Hsiao, Y. H. Lan, P. Y. Lee, T. L. Chiu, J. H. Lee, *Org. Electron.* **2011**, *12*, 547.
[17] J. H. Jou, P.-Y. Hwang, W.-B. Wang, C.-W. Lin, Y.-C. Jou, Y.-L. Chen, J.-J. Shyue, S.-M. Shen, S.-Z. Chen, *Org. Electron.* **2012**, *13*, 899.
[18] S. Lamansky, P. Djurovich, D. Murphy, F. Abdel-Razzaq, H.-E. Lee, C. Adachi, P. E. Burrows, S. R. Forrest, M. E. Thompson, *J. Am. Chem. Soc.* **2001**, *123*, 4304.
[19] J. P. Duan, P. P. Sun, C. H. Cheng, *Adv. Mater.* **2003**, *15*, 224.
[20] Z. B. Wang, M. G. Helander, J. Qiu, D. P. Puzzo, M. T. Greiner, Z. W. Liu, Z. H. Lu, *Appl. Phys. Lett.* **2011**, *98*, 073310.

[21] Y. Kawamura, K. Goushi, J. Brooks, J. J. Brown, H. Sasabe, C. Adachi, *Appl. Phys. Lett.* **2005**, *86*, 071104.
[22] L. X. Xiao, Z. J. Chen, B. Qu, J. X. Luo, S. Kong, Q. H. Gong, J. Kido, *Adv. Mater.* **2011**, *23*, 926.
[23] S. Reineke, K. Walzer, K. Leo, *Phys. Rev. B* **2007**, *75*, 125328.
[24] D. D. Song, S. L. Zhao, Y. C. Luo, H. Aziz, *Appl. Phys. Lett.* **2010**, *97*, 243304.
[25] Z. D. Popovic, H. Aziz, *J. Appl. Phys.* **2005**, *98*, 013510.
[26] Y.-L. Chang, Z. B. Wang, M. G. Helander, J. Qiu, D. P. Puzzo, Z. H. Lu, *Org. Electron.* **2012**, *13*, 925.
[27] M. A. Baldo, C. Adachi, S. R. Forrest, *Phys. Rev. B* **2000**, *62*, 10967.
[28] Y. Sun, S. R. Forrest, *Nat. Photonics* **2008**, *2*, 483.
[29] T. Förster, *Discuss. Faraday Soc.* **1959**, *27*, 7.
[30] F. S. Steinbache, R. Krause, A. Hunze, A. Winnacker, *Phys. Status Solidi A* **2011**, *209*, 340.
[31] G. D. Scholes, *Annu. Rev. Phys. Chem.* **2003**, *54*, 57.
[32] D. Guo, T. E. Knight, J. K. McCusker, *Science* **2011**, *334*, 1684.
[33] D. L. Huber, *Phys. Rev. B* **1979**, *24*, 893.
[34] W. S. Jeon, T. J. Park, S. Y. Kim, R. Pode, J. Jang, J. H. Kwon, *Org. Electron.* **2009**, *10*, 240.
[35] Y. R. Sun, S. R. Forrest, *Appl. Phys. Lett.* **2007**, *91*, 263503.
[36] S. L. Lai, S. L. Tao, M. Y. Chan, T. W. Ng, M. F. Lo, C. S. Lee, X. H. Zhang, S. T. Lee, *Org. Electron.* **2010**, *11*, 1511.
[37] X. F. Qi, M. Slootsky, S. Forrest, *Appl. Phys. Lett.* **2008**, *93*, 193306.
[38] S. L. Gong, Y. H. Chen, J. J. Luo, C. L. Yang, C. Zhong, J. G. Qin, D. G. Ma, *Adv. Funct. Mater.* **2011**, *21*, 1168.
[39] X. H. Yang, F. I. Wu, H. Haverinen, J. A. Li, C. H. Cheng, G. E. Jabbour, *Appl. Phys. Lett.* **2011**, *98*, 033302.
[40] Z. M. Hudson, C. Sun, M. G. Helander, H. Amarne, Z. H. Lu, S. N. Wang, *Adv. Funct. Mater.* **2010**, *20*, 3426.
[41] Z. M. Hudson, M. G. Helander, Z. H. Lu, S. N. Wang, *Chem. Commun.* **2011**, *47*, 755.
[42] M. Hashimoto, S. Igawa, M. Yashima, I. Kawata, M. Hoshino, M. Osawa, *J. Am. Chem. Soc.* **2011**, *133*, 10348.
[43] S. R. Forrest, D. D. C. Bradley, M. E. Thompson, *Adv. Mater.* **2003**, *15*, 1043.
[44] Y. Kawamura, H. Sasabe, C. Adachi, *Jpn. J. Appl. Phys.* **2004**, *43*, 7729.